

## 통합최적프레임을 사용한 광부상헤드를 탑재한 서스펜션의 최적화

### Design and Optimization of Suspension with Optical Flying Head Using Integrated Optimization Frame

김지원<sup>†</sup>, 박경수<sup>\*</sup>, 윤상준<sup>\*\*</sup>, 최동훈<sup>\*\*</sup>, 박영필<sup>\*\*\*</sup>, 이종수<sup>\*\*\*</sup>, 박노철<sup>\*\*\*\*</sup>

Ji-Won Kim, Kyoung-Su Park, Sang-Joon Yoon, Dong-Hoon Choi, Young-Pil Park, Jong-Soo Lee, and No-Cheol Park

#### Abstract

This paper optimizes the optical flying head (OFH) suspension using the integrated optimization frame, which automatically integrates the analysis with the optimization and effectively implements the repetitive works between them. The problem formulation for the optimization is suggested to improve the dynamic compliance of OFH and to shift the resonant frequencies caused tracking errors to high frequency domain. Furthermore, the minimization of the effective suspension mass that leads to decrease the so-called "lift-off" as the disk-head separation acceleration divided by the suspension load is taken into consideration. In particular, this study is carried out the optimal design considering the process of modes tracking through the entire optimization processes. The advanced suspension that reduces the effective mass of the suspension and increases the resonant frequencies of sway and 2<sup>nd</sup> torsion over 10kHz is achieved by using the integrated optimization frame.

**Key Words:** Optimization, Optical Flying Head Suspension, Integrated Optimization Frame, Mode Tracking

#### 1. Introduction

The optical systems using the probe and solid immersion lens (SIL) have been researched as the technology to embody the near field recording (NFR). Most of them use the flying head mechanism to accomplish a large capacity, a high data transfer rate and a high anti-shock resistance. The rotary actuator with OFH has better dynamic performances than common pick-up because of a rigid body structure and small weight of moving part. To achieve a higher track density, off-track errors of the flying head using the rotary actuator must be reduced because they make the read/write errors happen in case of a narrower track pitch, especially. Sources of off-track errors are mechanical

resonance, spindle runout, external vibration, servo track writer (STW) error, and so on. It is obvious that a higher bandwidth servo system can easily correct these errors, and enable precision positioning of the flying heads. Therefore, the suspension, including the flying head, must have higher resonant frequencies in the access direction (i.e. the radial in-plane direction).[1] On the other hand, the flexure part of the suspension has better resilience to carry read/write signals flexibly. For these reasons, we consider the cantilever mode as the compliance mode that has an effect on resilience of the flying head. In particular, increasing flexibility will generally reduce the flying height modulation in the operating condition. And it helps the flying stability of OFH remain on disk surface. Then, it is very difficult to design a more flexible flexure without decreasing high resonant frequencies such as sway and 2nd torsion. A better understanding of dynamic characteristics of OFH is essential. In addition, "head slap" due to shock loading is becoming an increasingly important issue for using flying head system. In this paper, we measure the effective mass, which determines the "disk-head separation acceleration" as a value for shock resistance about the head-suspension of OFH with gram load.[2] All characteristics for the suspension with optical flying

<sup>†</sup> Graduate School of Mechanical Engineering, Yonsei Univ.  
E-mail : jiwon\_kim@yonsei.ac.kr

<sup>\*</sup> Graduate School of Mechanical Engineering, Yonsei Univ.

<sup>\*\*</sup> Center for Innovative Design Optimization Technology,  
Hanyang Univ.

<sup>\*\*\*</sup> Department of Mechanical Engineering, Yonsei Univ.

<sup>\*\*\*\*</sup> Center for Information Storage Devices.

논문접수일 (2005년 4월 3일)

head are optimized using integrated optimization frame, which automatically integrates the analysis with the optimization and effectively implements the repetitive works between analysis, design and optimization processes. In this study, ModelCenter™ is used for the integrated optimization tool.

## 2. OFH Suspension Analysis

### 2.1 Initial Model and Design Variables for OFH

Fig. 1 shows the initial shape of the suspension and design variables used in this study. It is an integrated type in order not to interrupt an optical path. The number of design variables including the thickness is 15 totally. And the length between the center of pivot and SIL is fixed at 13.0mm and tool hole is off 6.5mm from SIL's center considering the specification of an actuator suitable to lynch disk drive. The bound of suspension's thickness is determined from 0.4mm to 1.0mm considering the fabrication and dynamic performance. Besides, the bent angle is changed by the calculated the vertical stiffness each step and the initial value is 16 deg. We checked the sensitivities for upper 15 design variables performing the parametric studies. 5 design variables that affect very small compared with other design variables were fixed. Those fixed design variables are *cir\_length\_1*, *cir\_length\_2*, *f\_width*, *f\_length* and *hole\_length*. In this paper, we optimized using 10 design variables except upper 5-fixed design variables.

### 2.2 Mode Tracking Method

The easiest correlation check is the comparison of natural frequencies and mode shapes between systems. For the reason, a lot of correlation methods are used widely in various research areas. In particular, the modal assurance criterion (MAC) method is typically used in the correlation check problem. MAC is a correlation for each pair of a reference and modified mode shape :

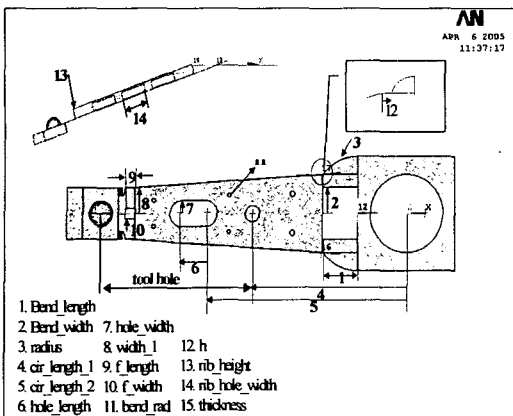


Fig. 1 Suspension type and design variables

$$MAC(i,j) = MAC(\{\phi_i^c\}, \{\phi_j^m\}) = \frac{|\{\phi_i^c\}^T \{\phi_j^m\}|^2}{(\{\phi_i^c\}^T \{\phi_i^c\})(\{\phi_j^m\}^T \{\phi_j^m\})} \quad \left\{ \begin{array}{l} i=1, \dots, N_m^c \\ j=1, \dots, N_m^m \end{array} \right. \quad (1)$$

$\{\phi_i^c\}$  Eigen-vector matrix of reference modes

$\{\phi_j^m\}$  Eigen-vector matrix of modified modes

$N_m^c$  Number of reference modes

$N_m^m$  Number matrix of modified modes

MAC values always lie between 0 and 1. A MAC value equal to 1 indicates a very good correlation. A MAC value equal to 0 indicates that the two modes do not show any correlation. In case the bound of design variables is infinitesimal, there is no problem to use the MAC method because the interruption between detecting points in two models doesn't happened. However, when design variables change widely, it is not suitable to compare with the correlation between mode shape of the reference model and modified model using this MAC method on account of the interruption between detecting points.[3] The phenomenon is been able to explain through Fig. 2. Therefore, the comparison using MAC method misunderstands or doesn't distinguish each mode shape because the eigenvectors for same nodes aren't identified as shown in Fig. 2. This study proposes a new mode tracking method aimed to accurately distinguish the mode shapes between modified and reference models. Most engineering systems are continuous and have an infinite number of degrees of freedom. There are [n] natural frequencies, each associated with its own mode shape, for a system having [n] degrees of freedom. The method of determining the natural frequencies forms the

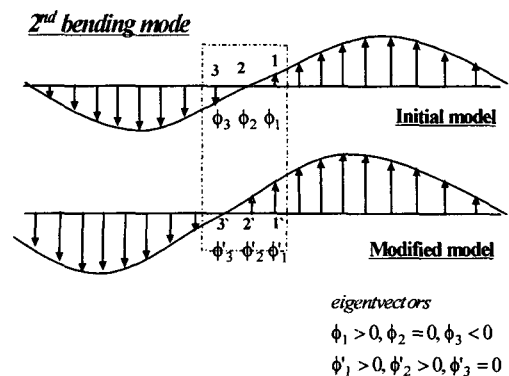


Fig. 2 Misunderstanding of eigen-value

characteristic equation. It can be described as the matrix form;

$$[M]\{\ddot{x}(t)\} + [K]\{x(t)\} = \{f(t)\} \quad (2)$$

$$[M]\{\ddot{x}(t)\} + [K]\{x(t)\} = \{0\} \quad (3)$$

Assumed solution as synchronous motion:

$$\{x(t)\} = \{X\}e^{i\Omega t} \quad \{-\Omega^2[M] + [K]\}\{X\} = \{0\} \quad (4)$$

Eigen-value and corresponding eigenvectors are

$$\Omega_r, \{\phi_r\}, (r = 1, 2, \dots, N)$$

$$\Omega_r^2 \{\phi_r\}^T [M] \{\phi_r\} = \{\phi_r\}^T [K] \{\phi_r\}$$

$$(\Omega_r^2 - \Omega_s^2) \{\phi_s\}^T [M] \{\phi_r\} = 0 \quad \Omega_r^2 \neq \Omega_s^2 \text{ then } \{\phi_s\}^T [M] \{\phi_r\} = 0 \\ \text{then } \{\phi_s\}^T [K] \{\phi_r\} = 0 \quad (5)$$

Modal matrix is  $[\Phi] = [\{\phi_1\}, \{\phi_2\}, \dots, \{\phi_N\}]$

where,  $\{\phi_i\}$  is the eigen-vector matrix for  $i$  mode shape. These eigen-vectors determine the mode shape for each mode frequency. When eigen-vector is almost zero at the detecting nodes, the line that links these points is called the nodal line.[4] And the mode shapes are distinguished by this characteristic. We can distinguish the mode shapes using the number of nodal line excluding fixing line is zero, the mode is one among cantilever, 1<sup>st</sup> torsion and sway mode in suspension system. And in case the value is one, they indicate either 1<sup>st</sup> bending or 2<sup>nd</sup> torsion mode. After some modes are classified by this process, we are carried out one more process in order to subdivide each mode. It examines the multiplication between eigen vectors at both ends (A, B) of OFH as shown in Fig. 4. If the value is negative, it means that the mode is concerned with torsion mode. Otherwise, it represents that it is similar to the bending mode. Through these processes, we can investigate the correlation between the mode shapes of the reference and modified model during the optimization process.

### 3. Optimal Design for OFH Suspension

#### 3.1 Integration and Optimization Method

Numerical search routines are used to drive the integrated model to explore the design space effectively. ModelCenter™ uses unique integrated architecture with another module called “Analysis Server” to wrap and integrate legacy programs, data, and geometry features. Fig. 5 shows our model linked within ModelCenter™. Furthermore, ModelCenter™ contains gradient-based optimization algorithms that can be used with any model or combination of models in the system. And the optimization routines can quickly search the feasible

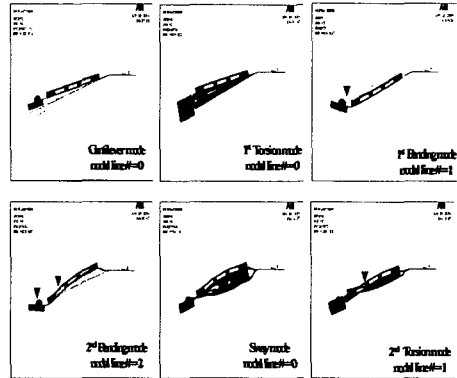


Fig. 3 Number of nodal line for each mode

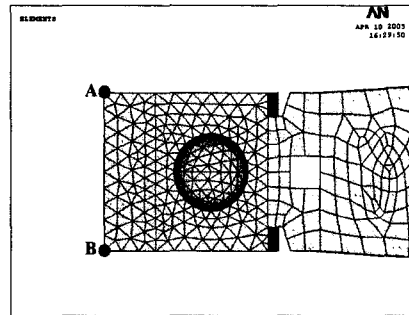


Fig. 4 Detecting node points for distinction of torsion and bending mode

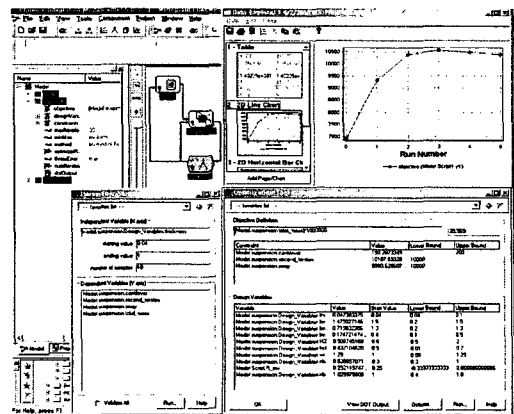


Fig. 5 Integrated optimization Frame

design space and find optimal parameters[5]. In this study, we use the modified method of feasible direction (MMDF) for the optimization method. The modified method of feasible direction is a nonlinear programming technique, which uses the usable-feasible direction  $S$  to reduce the objective function value without violating the active constraints for some small finite movement. Having determined the search direction,

constrained line search is performed to find the optimal distance  $\alpha^*$  along the usable-feasible direction. Then, the design variable vector  $X$  is updated as

$$X^q = X^{q-1} + \alpha^* S^q \quad (6)$$

,where  $q$  is the number of iterations for optimization. As previously stated, there are many design specifications, which have to be considered in the design of suspension with OFH. This study performs 3 different steps of the optimization to satisfy all the requirements for the suspension design. At first, we optimize the suspension only considering the compliance mode frequency and resonant frequencies in the access direction. Secondly, aimed to consider the effective mass, we make a different formulation of optimization using the first optimal model. But the formulation is not wholly different from the first one. Because the constraints used in the first optimization process were kept equally during the optimization to minimize effective mass is performed. Finally, we perform another analysis to consider the tolerance of fabrication. Those design processes using 3 different steps are complicated and inconvenient. But we can easily check the available limit performances of our model. And also, we can verify the shapes of model in each optimization step to have appropriate performances. Therefore, we can find out a good optimal solution faster and easier than common one step optimization process. And the integrated optimization frame systematically carries out all those results.

### 3.2 Optimization Considering Servo Bandwidth

As mentioned before, the suspension, including the flying head, must have higher resonant frequencies in the access direction (i.e. the radial in-plane direction). And also it must have better resilience. The initial model of this paper has only one compliance mode, which is the cantilever mode. We designate sway and 2<sup>nd</sup> torsion to the resonant frequencies that have to shift toward high frequency domain to avoid the tracking errors. Fig 6 shows the mode shapes of cantilever, 2<sup>nd</sup> torsion and sway respectively. Each mode frequency of the initial model is represented in Table 1. As explained before, the formulation for the first optimization is composed to increase the mode frequencies of 2<sup>nd</sup> torsion and sway and keep the mode frequency for cantilever under an appropriate range. The objective function and constraints are shown from Eq.(7) to Eq. (10)

Table 1 Mode Frequencies of Initial Model

Cantilever	2 <sup>nd</sup> Torsion	Sway
105.3Hz	6920Hz	7880.9Hz

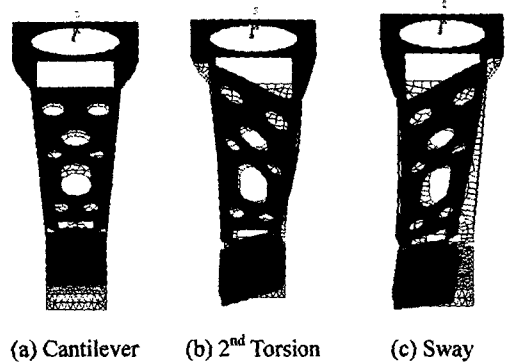


Fig. 6 Mode Shapes of the initial model

$$\begin{aligned} &Max, Min f(x) \\ &f(x) = (2^{nd} \text{ torsion}, \text{ Sway}) \end{aligned} \quad (7)$$

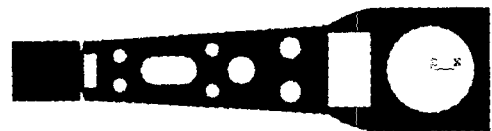
Subject to

$$\text{Cantilever} \leq 0.2kHz \quad (8)$$

$$2^{nd} \text{ torsion} \geq 10kHz \quad (9)$$

$$\text{Sway} \geq 10kHz \quad (10)$$

As shown in Eq. (7), the objective function is formulated by the *Max, Min* problem. And the objective function distinguishes the less value between 2<sup>nd</sup> torsion and sway firstly. Then the optimization proceeds to the direction for maximizing the less value. In particular, the distinction process is performed every time when the gradient changes to decide the search direction. Fig. 7 and Table 2 show the comparison of the mode shapes and the change of design variables between the initial model and the optimal model for this optimization.



(a) Initial Model (frontal view)



(b) Optimal Model (frontal view)

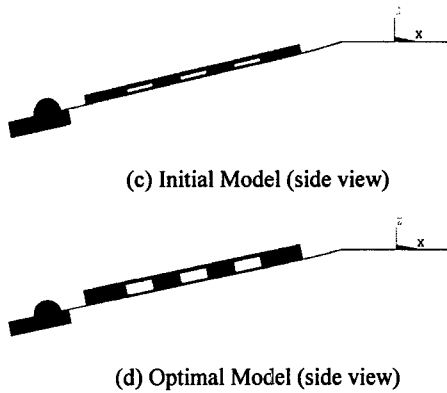


Fig. 7 Comparison shapes between initial and optimal mode

Table 2 Changes of design variable between initial and optimal model

Design Variables	Initial (mm)	Optimal (mm)
Thickness	0.04	0.05396
Bend_Length	1.5	1.47855
Bend_Width	1.3	0.99643
Bend_Rad	0.4	0.13675
H	0.6	0.61569
Hole_Width	0.5	0.23283
Width	1	1.29
Rib_Height	0.3	0.55986
Radius	4	4.34265
Rib_Hole_Width	1	1.01177

Table 3 Comparison mode frequencies between Initial and optimal model

	Initial	Optimal	Improvement
Cantilever	105Hz	200Hz	-47.5%
2 <sup>nd</sup> Torsion	6920Hz	11064Hz	37.5%
Sway	7880Hz	10390Hz	24.2%

Table 3 and Fig. 8 show the variation of three mode frequencies between the initial model and the optimal model. As shown in the Table 3 and Fig. 8, we can recognize that all the constraints of this optimization are

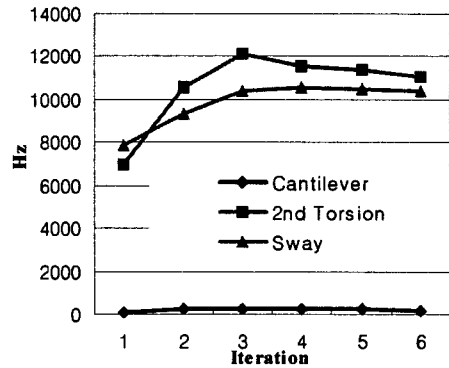


Fig. 8 Variation of 3 mode frequencies

satisfied and the mode change is occurred in the optimization process.

### 3.3 Optimization Considering Effective Mass

Shock resistance becomes a greater problem in small form factor (SFF) optical storage devices. Generally, the external shock acceleration that causes head-disk interface (HDI) failures is related to the acceleration that causes the head-disk separation[6]. Eq. (11) gives the relationships between slider mass, suspension equivalent mass, head-disk separation acceleration ( $a_s$ ), and load force on the slider ( $F$ ). The effective mass ( $M_{eff}$ ) is composed by the sum of slider mass and equivalent mass. Here, the suspension equivalent mass is the effective mass to determine the spring rate of the suspension.

$$a_s = F / M_{eff} \quad (11)$$

This equation means that the smaller suspension equivalent mass and slider masses, and larger load force are good to achieve higher external shock resistance in the head suspension assembly. However, the larger load force reduces the HDI durability against stiction and wear between the disk and slider during contact start stop (CSS). Therefore, in this paper, we fix the external force to 3gf and reduce the effective mass to increase the head-disk separation acceleration.

$$\begin{aligned} \text{Min } & f(x) \\ & f(x) = (M_{effective}) \end{aligned} \quad (12)$$

Subject to

$$\text{Cantilever} \leq 0.2\text{kHz} \quad (13)$$

$$2^{nd} \text{ torsion} \geq 10\text{kHz} \quad (14)$$

$$\text{Sway} \geq 10\text{kHz} \quad (15)$$

As mentioned before, the optimal model that is optimized at chapter 3.2 is used as the initial model of this optimization (named: New Initial Model) and the constraints are same as the formulation of chapter 3.2. Fig. 9 and Table 4 show the comparison of the shapes and the design variables changing between the new initial model and the optimal model for this optimization..

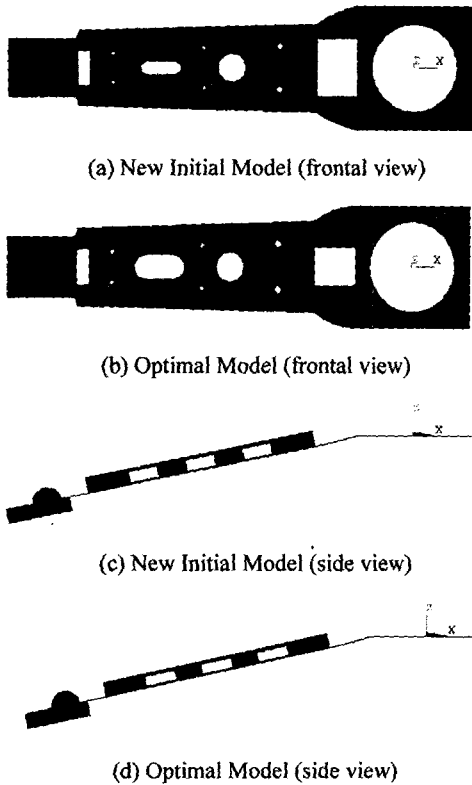


Fig. 9 Comparison shapes between new initial and optimal model

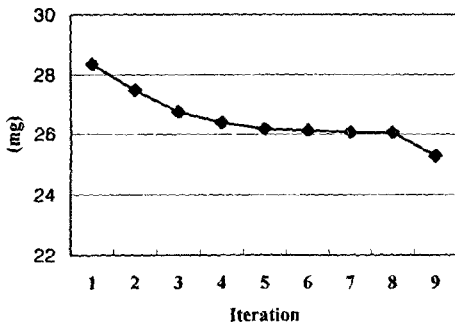


Fig. 10 Variation of effective mass

Table 4 Changes of design variable between new Initial and optimal model

Design Variables	New Initial (mm)	Optimal (mm)
Thickness	0.05396	0.04667
Bend_Length	1.47855	1.5
Bend_Width	0.99643	0.63586
Bend_Rad	0.13675	0.15409
H	0.61569	0.50633
Hole_Width	0.23283	0.40185
Width	1.29	1.29
Rib_Height	0.55986	0.48962
Radius	4.34265	2.5626
Rib_Hole_Width	1.01177	1.09192

Table 5 Comparison mode frequencies between new initial and optimal model

	New Initial	Optimal	Improvement
Cantilever	200Hz	195Hz	2.6%
2 <sup>nd</sup> Torsion	11064Hz	10217Hz	-8.3%
Sway	10390Hz	10000Hz	-3.9%
M <sub>ef</sub>	28.35mg	25.27mg	12.2%

Table 5 shows the variation of three mode frequencies and effective mass between the new initial model and the optimal model. As shown in the Table 5, we can recognize that all the constraints of this optimization are satisfied and the effective mass is reduced with an improvement of 12.2%. And Fig. 10 shows the variation of the effective mass during the optimization process.

### 3.4 Modification and Verification for Fabrication

The tolerance for the fabrication should be considered in the design process because we consider the tolerance of a machine tool and cost of fabrication. In this study, through the parametric studies and optimization process, we recognized that the thickness was the most sensitive design factor in the suspension. And also, the thickness is the most effective term that decides such as the cost of fabrication and so on. Therefore, we round off the thickness to three decimal places and optimize again to follow the formulation of

Eq. (12)~(15). After that, we round off all design variables to each appropriate value. Fig. 11 and Table 6 show the comparison of the shapes and the design variables changing between the initial model and the final model.

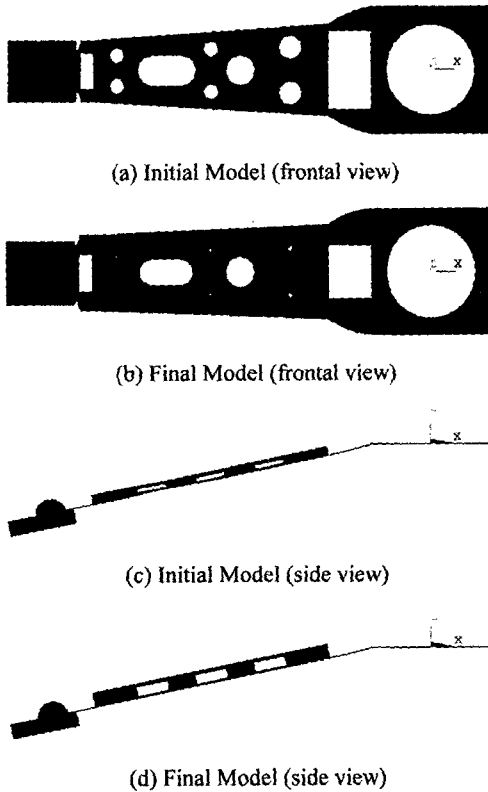


Fig. 11 Comparison shapes between initial and final model

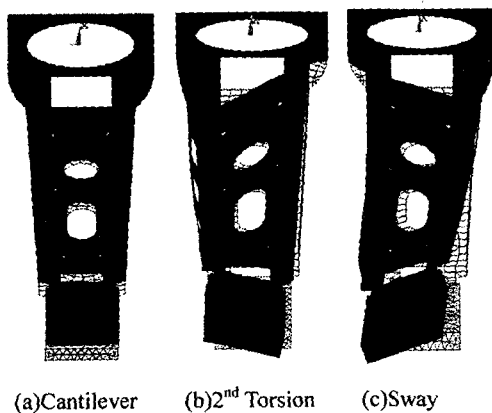


Fig. 12 Three mode shapes of the final model

Table 6 Changes of design variable between original and final model

Design Variables	Initial (mm)	Final (mm)
Thickness	0.04	0.05
Bend_Length	1.5	1.5
Bend_Width	1.3	0.852
Bend_Rad	0.4	0.1
H	0.6	0.5
Hole_Width	0.5	0.423
Width	1	1.195
Rib_Height	0.3	0.5
Radius	4	2.84
Rib_Hole_Width	1	1.085

Table 7 Comparison mode frequencies and effective mass

	Cantilever	2 <sup>nd</sup> Torsion	Sway	M <sub>eff</sub> (mg)
Initial	105Hz	6920Hz	7880Hz	20.57
1 <sup>st</sup> Optimal	200Hz	11064Hz	10390Hz	28.35
2 <sup>nd</sup> Optimal	195Hz	10217Hz	10000Hz	25.27
Final	195Hz	10356Hz	10000Hz	25.79

Table 7 shows the variation of three mode frequencies and effective mass from the new initial model to the final model. '1<sup>st</sup> Optimal' values and '2<sup>nd</sup> Optimal' values in the Table 7 are the results of using formula Eq. (7)~Eq. (10) and using formula Eq. (12)~Eq. (15) respectively. And the 'Final' values in the Table 7 are the results that are considered the tolerance for the fabrication on each design variable. As shown in the Table 7, we can recognize that all the constraints of this optimization are satisfied and the effective mass is reduced with an improvement about 10% comparing with the first optimal model that is performed to consider only resonant frequencies for three mode shapes. Fig 12 shows the mode shapes of cantilever, 2<sup>nd</sup> torsion and sway respectively. As shown in the Fig. 12, all mode shapes are kept the original mode shapes. For this reason, we can check and verify about the accuracy of the mode tracking process used in this study.

#### 4. Conclusions

We have proposed a new integrated suspension with optical flying head. The advanced suspension designed in this study, features a resilient monolithic body that includes a load beam and bending region and flexure part. Through many processes, the advanced design for OFH suspension is achieved. The effective mass of the advanced suspension is about 12.2% as light as the suspension that is considered only resonant frequencies for three mode shapes. Due to this reason, the head-disk separation acceleration is about 9% as high as the suspension that is considered only resonant frequencies. In addition, the advanced suspension keeps the resonant frequencies of sway and 2<sup>nd</sup> torsion over 10kHz and the resonant frequency of cantilever under 0.2kHz. The amounts of the improvement for sway and 2<sup>nd</sup> torsion between initial and final model are 33.2% and 21.2% respectively.

#### Acknowledgments

This work was funded by the Korea Science and Engineering Foundation (KOSEF) through the Center for Information Storage Device (CISD) Grant No. R11-1997-042-11001-0. And This research was supported by Center of Innovative Design Optimization Technology (IDOT, ERC of Korea Science and Engineering Foundation).

#### Reference

- [1] T. Watanabe, T. Ohwe, S. Yoneoka, and Y. Mizoshita, 1997, "An Optimization Method for Precision Positioning of Pico-CAPS", IEEE TRANSACTIONS ON MAGNETICS, Vol.33, No.5
- [2] Chih-Wu Jen and Frank E. Talke, Takeshi Ohwe, Alan Gordon, 1997, "On Suspension Dynamics for Pico-Sliders", IEEE TRANSACTIONS ON MAGNETICS, Vol.33, No.5
- [3] Henry Ng, Suleyman Guleyupoglu, Frank Segaria, Barrett Malone, Scott Woyak, et al, 2003, "Collaborative Engineering Enterprise with Integrated Modeling Environment", Euro-Simulation Interoperability Workshop, Stockholm, Sweden, pp. 03E-SIW-034
- [4] S.K. Yu and B. Liu, 2003, "Optimal Suspension Design for Femto Sliders", IEEE Transactions on magnetics, Vol.39, No.5
- [5] Yoon, Gil Ho and Yoon Young Kim, 2002, "Topology Optimization of Optical Pickup Suspension Plates", Proceeding of the ninth AIAA/ISSMO Symposium on Multidisciplinary Analysis and Optimization.
- [6] T. Ohwe, T. Watanabe, S. Yoneoka and Y. Mizoshita, 1996, "a New Integrated Suspension for PICO-SLIDER", IEEE TRANSACTIONS ON MAGNETICS, Vol.32, No.5